Atmos. Chem. Phys. Discuss., 12, 21065–21104, 2012
www.atmos-chem-phys-discuss.net/12/21065/2012/
doi:10.5194/acpd-12-21065-2012

Atmospheric Chemistry and Physics Discussions

Diurnal variation of stratospheric HOCl, ClO and HO_2 at the equator: comparison of 1-D model calculations with measurements of satellite instruments

M. Khosravi[1], P. Baron[2], J. Urban[1], L. Froidevaux[3], A. I. Jonsson[4], Y. Kasai[2,5], K. Kuribayashi[2,5], C. Mitsuda[6], D. P. Murtagh[1], H. Sagawa[2], M. L. Santee[3], T. O. Sato[2,5], M. Shiotani[7], M. Suzuki[8], T. von Clarmann[9], K. A. Walker[4], and S. Wang[3]

[1]Department of Earth and Space Sciences, Chalmers University of Technology, Gothenburg, Sweden
[2]National Institute of Information and Communications Technology, Tokyo, Japan
[3]Jet Propulsion Laboratory, California Institute of Technology, Pasadena, CA, USA
[4]Tokyo Institute of Technology, Kanagawa, Japan
[5]Tokyo Institute of Technology, Yokohama, Japan
[6]Fujitsu FIP Corporation, Tokyo, Japan
[7]Research Institute for Sustainable Humanosphere, Kyoto University, Kyoto, Japan
[8]Japan Aerospace Exploration Agency, Ibaraki, Japan

[9]Karlsruhe Institute of Technology, Institute for Meteorology and Climate Research, Karlsruhe, Germany

Received: 10 May 2012 – Accepted: 20 July 2012 – Published: 20 August 2012

Correspondence to: M. Khosravi (maryam.khosravi@chalmers.se)

Published by Copernicus Publications on behalf of the European Geosciences Union.

ACPD
12, 21065–21104, 2012

Abstract

The diurnal variation of HOCl and the related species ClO, HO_2 and HCl measured by satellites has been compared with the results of a one-dimensional photochemical model. The study compares the data from various limb-viewing instruments with model simulations from the middle stratosphere to the lower mesosphere. Data from three sub-millimeter instruments and two infrared spectrometers are used, namely from the Sub-Millimeter Radiometer (SMR) on board Odin, the Microwave Limb Sounder (MLS) on board Aura, the Superconducting Submillimeter-wave Limb-Emission Sounder (SMILES) on the International Space Station, the Michelson Interferometer for Passive Atmospheric Sounding (MIPAS) on board ENVISAT, and the Atmospheric Chemistry Experiment Fourier Transform Spectrometer (ACE-FTS) on board SCISAT. Inter-comparison of the measurements from instruments on sun-synchronous satellites (SMR, MLS, MIPAS) and measurements from solar occultation instruments (ACE-FTS) is challenging since the measurements correspond to different solar zenith angles (or local times). However, using a model which covers all solar zenith angles and the new SMILES instrument which measures at all local times over a period of several months provides the possibility to indirectly compare the diurnally variable species. The satellite data were averaged for latitudes of 20° S to 20° N for the SMILES observation period from November 2009 to April 2010 and were compared at three altitudes: 35, 45 and 55 km. This study presents the first evaluation of HO_2 Odin/SMR data and also the first comparison of the new SMILES data and the latest version of MLS (version 3.3) with other satellite observations. The *MISU-1D* model has been run for conditions and locations of the observations. The diurnal cycle features for the species investigated here are generally well reproduced by the model. The satellite observations and the model generally agree well in terms of absolute mixing ratios as well as differences between the day and night values. This confirms that gas phase chemistry of these species based on latest recommendations of reaction rate constants is fairly well understood.

ACPD

12, 21065–21104, 2012

1 Introduction

Hypochlorous acid, HOCl, is considered to be a reservoir for active chlorine, ClO_x, and odd hydrogen, HO_x, in the stratosphere (von Clarmann et al., 2012). It is produced primarily by the reaction of ClO and HO_2 (peroxy radical) and is destroyed mainly by photo-dissociation at the wavelengths shorter than 420 nm which returns OH and Cl radicals (Hickson et al., 2007).

$$ClO + HO_2 \rightarrow HOCl + O_2 \quad \text{(R1)}$$

$$HOCl + h\nu \rightarrow Cl + OH \quad \text{(R2)}$$

There are other pathways for the destruction of HOCl, through reactions with atomic chlorine, OH radicals and atomic oxygen, however these reactions are minor mechanisms (Chance et al., 1989). Furthermore, in the polar vortices HOCl is generated by heterogeneous chemistry and contributes to the polar ozone loss events (Hanson and Ravishankara, 1992; Abbatt and Molina, 1992). Since Reaction (R1) is the most important gas phase reaction leading to the formation of stratospheric HOCl, model calculations are sensitive to the rate constant, k_1, of this reaction. There have been number of studies attempting to determine k_1 at room temperature (Reimann and Kaufman, 1978; Leck et al., 1980; Burrows and Cox, 1981). Additionally, some studies have reported a temperature dependence of the rate coefficient (Stimpfle et al., 1979; Nickolaisen et al., 2000; Knight et al., 2000). However, there is a large discrepancy in the laboratory measurements of k_1, which can lead to disagreement between modelled and measured HOCl. Kovalenko et al. (2007) reported that the value of k_1 published by Stimpfle et al. (1979) is a factor of two faster than JPL 2006 recommendations (Sander et al., 2006) and is more consistent with their measurements. The conclusion of Kovalenko et al. (2007), based on two balloon-borne instruments (FIRS-2, Far-InfraRed emission Spectrometer and MkIV, mid-infrared solar absorption spectrometer), has been confirmed by von Clarmann et al. (2009). The Stimpfle et al. (1979) formula for calculation of the rate constant is based on non-Arrhenius behavior of the rate coefficient with strong

ACPD
12, 21065–21104, 2012

negative temperature dependency, while JPL 2006 (Sander et al., 2006) to JPL 2011 (Sander et al., 2011) use a standard Arrhenius expression.

There have been a variety of stratospheric measurements of HOCl. von Clarmann et al. (2009) have summarized HOCl measurements made so far from balloon-, space- and airborne infrared solar absorption observations (Larsen et al., 1985; Toon et al., 1992; Raper et al., 1987), balloon-borne infrared and far infrared limb-viewing emission measurements (Chance et al., 1989; Johnson et al., 1995; von Clarmann et al., 1997) and satellite measurements. Global HOCl observations were first provided by the Michelson Interferometer for Passive Atmosphere Sounding (MIPAS) (von Clarmann et al., 2006) and further by the Microwave Limb Sounder (MLS) on board the Aura satellite (Waters et al., 2006). More recently, the Superconducting Submillimeter-wave Limb-Emission Sounder (SMILES) provided observations of the vertical distribution and diurnal variation of HOCl (Kikuchi et al., 2010). The ClO diurnal and seasonal variation measured by MLS on board the UARS satellite observations was provided by Ricaud et al. (2000) from year 1991 to 1997 in the mid-latitude range (40–50° N) and compared with the results from a zero-dimensional photochemical model as well as a three-dimensional chemical transport model. Sato et al. (2012) have recently compared these 7 yr average UARS data with the ClO mid-latitude diurnal variation from SMILES (January to February 2010) in the stratosphere and mesosphere.

In this paper we compare the results of a one-dimensional (1-D) photochemical model with concentrations of HOCl, ClO, HO_2 and HCl measured by Odin/SMR, Aura/MLS, MIPAS, ACE-FTS and SMILES in the tropical middle stratosphere to lower mesosphere altitude region. We investigate the diurnal variation of the species at low latitudes and at the altitudes of 35, 45 and 55 km during the period of SMILES observation from November 2009 to April 2010. Here, otherwise noted, the measured profiles, between 20° S and 20° N, were interpolated onto a fine altitude grid, binned into about 2.5–3° wide bins of solar zenith angle, and averaged over one month.

Data from new sub-millimeter instruments became available in the last decade with the launch of Odin in 2001, MLS in 2004 and finally SMILES in 2009. This paper aims

ACPD
12, 21065–21104, 2012

to compare the results of these fairly new sub-millimeter instruments with each other and with model simulations. In particular, HO_2 data from Odin/SMR has not been compared with other observations before and hence this paper represents the first validation of SMR HO_2 data. The inter-comparison of sun-synchronous satellite measurements (Aura/MLS and Odin/SMR) is a difficult and rather uncertain task, since such instruments measure at different solar zenith angles. The modeling of diurnal cycles of species provides a means of indirectly comparing these observations. The quality of the model is assessed by comparison with diurnal cycles from SMILES. Moreover, in the lower stratosphere (below 30 km), HO_2 reacts with NO and is converted to OH and NO_2, which dominates over Reaction (R1) (Jucks et al., 1998). Therefore, the diurnal variations of HO_2 and HOCl are studied only from the middle stratosphere to the lower mesosphere, where the interference with NO is minimal. The model as a reference helps to better understand and confirm the kinetics of the reactions involved.

The satellite measurements used in this study are described in Sect. 2. Section 3 provides details on the model and the simulations of HOCl, ClO, HO_2 and HCl. The results of the satellite and model comparisons as well as a study of HOCl reaction rates are presented in Sect. 4. Conclusions are provided in Sect. 5.

2 Measurements

The observations are described in two subsections corresponding to the measurement method. Odin/SMR, Aura/MLS and SMILES are sub-millimeter limb sounding measurements, whilst MIPAS and ACE-FTS are thermal emission and solar occultation infrared limb-viewing measurements, respectively.

2.1 Sub-millimeter wave limb-viewing measurements

The Sub-Millimetre Radiometer (SMR) on the Odin satellite, launched in 2001, measures thermal emission at the atmospheric limb using various bands in the

ACPD
12, 21065–21104, 2012

486–581 GHz spectral region (Murtagh et al., 2002; Frisk et al., 2003). The satellite was launched in a sun-synchronous orbit crossing the equator at about 06:00 a.m. and 06:00 p.m. Due to the lack of fuel on board the satellite, the SMR equator crossing times changed slowly from 06:00 a.m. (06:00 p.m.) to almost 07:00 a.m. (07:00 p.m.) during the course of the mission as the orbit altitude decreased from about 620 to 580 km. We use Odin/SMR ClO and HO_2 level-2 data of version 2.1 of the operational processor. ClO was measured using a band centered at 501.8 GHz every second day during the relevant period November 2009 to April 2010. Vertical profiles are typically available between 15 to 65 km with a vertical resolution of 2.5–3 km up to roughly 45 km and degrading considerably above 45–50 km where the vertical sampling interval changes in this particular observation mode. A more detailed description of the ClO data set and an inter-comparison with coincident profile measurements made by Aura/MLS are provided by Urban et al. (2005, 2006) and Santee et al. (2008). HO_2 is measured in a band centered at 576.9 GHz. As the frequency of this radiometer is normally not stable due to a hardware failure (phase-lock) (Dupuy et al., 2004), only data for a short period from October 2003 to October 2004 are so far analyzed and used in this study. HO_2 measurements were performed on only one observation day per month. Baron et al. (2009) provides a description of the characteristics of the Odin/SMR HO_2 data set. In contrast to Baron et al. (2009), who used an off-line retrieval approach, we use the operational Odin/SMR single-profile retrieval product providing data between about 30 and 60 km with a vertical resolution varying from 4 to 8 km within this range. The operational HO_2 data have so far not been compared to other measurements.

The Microwave Limb Sounder (MLS) on board the Aura satellite has been operating since 2004. MLS has a sun-synchronous near-polar orbit and measures vertical profiles of various species from the upper-troposphere to the lower mesosphere in the millimeter and sub-millimeter spectral regions (Froidevaux et al., 2008; Santee et al., 2008; Pickett et al., 2008; Barret et al., 2006). We have used the version 3.3 products for HOCl, HCl, HO_2 and ClO. MLS measures the same spectral lines of HCl and ClO as SMILES (around 625 and 649 GHz, respectively). The vertical resolution is 3–6 km

ACPD
12, 21065–21104, 2012

for HOCl, 3–5 km for HCl, 3–4 km for ClO and 4–5 km for HO_2. The MLS data with negative error and bad quality have been removed according to the MLS user's guide documentation (Livesey et al., 2011). The MLS scientific team recommends HOCl data to be used only up to 2.2 hPa (~ 42 km) and ClO data up to 1 hPa (~ 48 km). We have, however, used the HOCl data at 45 km after removing the bad quality data. The MLS profiles in each solar zenith angle bin are averaged on pressure levels over one month. The averaged profile is interpolated onto a single geopotential altitude grid. The geopotential altitudes grid is calculated by averaging the geopotential altitudes measured by MLS during the period and the latitude considered in this analysis.

The Superconductive Submillimeter-wave Limb-Emission Sounder (SMILES) instrument was installed on the International Space Station (ISS) and used 4 K cooled superconductor detector technology to measure stratospheric and mesospheric species including HOCl, ClO, HO_2 and HCl (Kikuchi et al., 2010). The instrument was developed by the Japan Aerospace Exploration Agency (JAXA) and the National Institute of Information and Communications Technology (NICT). SMILES measured the vertical distribution of various stratospheric and mesospheric species from October 2009 until April 2010 mostly in the latitude range of 38° S–65° N (Kikuchi et al., 2010). Because of the 2-month precession of the ISS non-synchronous orbit, SMILES was able to follow the diurnal cycle of the chemical species. During one scan, two spectral bands are measured among the three pre-defined ones, named A (624.3–625.5 GHz), B (625.1–626.3 GHz) and C (649.1–650.3 GHz) (for more details, see the SMILES Mission Plan, version 2.1, at http://smiles.nict.go.jp/Mission_Plan/). In this paper, we use the data for the operational processor provided by JAXA version 2.1 (Mitsuda et al., 2011; Takahashi et al., 2010, 2011), here named SMILES-O. We also include the results from the research processor (version 2.1.5) developed by NICT, named here SMILES-R (Baron et al., 2011; Sato et al., 2012). Compared to the analyses presented in Baron et al. (2011), systematic errors in the level-2 data are reduced in these versions by taking into account the non-linearity of the radiometer gain in the spectral radiance calibration (level-1b version 7) and improvements of the spectroscopic database. The HOCl

ACPD
12, 21065–21104, 2012

profiles have a typical vertical resolution of 5, 8 and 14 km at 35, 45 and 55 km, respectively. The HO_2 profiles have an altitude resolution of about 4, 6, and 6 km for the same levels. The typical vertical resolution of ClO is about 4, 4 and 6 km. The altitude resolution of the $H^{37}Cl$ profile is 3, 4 and 6 km and that of $H^{35}Cl$ is 3, 3 and 5 km at 35, 45 and 55 km, respectively (Baron et al., 2011; Sato et al., 2012; Kasai et al., 2012).

2.2 Infrared limb-viewing observations

The Michelson Interferometer for Passive Atmospheric Sounding (MIPAS) was a mid-infrared limb-viewing emission spectrometer installed on the Environmental satellite (ENVISAT). ENVISAT was launched in 2002 into a sun-synchronous polar orbit (800 km) and stopped operation in April 2012. MIPAS took measurements by looking backwards and to the side for tangent altitudes from 6 to 68 km for the observation of stratospheric species. The vertical sampling of MIPAS was 3 km from 6 to 42 km and 8 km from 42 to 68 km. MIPAS acquired about 75–80 scans per orbit and a typical scan consisting of 15 to 17 limb-viewing measurements took about 70 s. ENVISAT crossed the equator with the ascending node at 10:00 and the descending node at 22:00 LT. The HOCl data used here are from the level 2 product processed at the Karlsruhe Institute of Technology. Due to some instrumental problems, MIPAS was operated at reduced spectral resolution since 2005 and no more HOCl data are available since then. Therefore, the HOCl data from MIPAS are taken from the period November 2003 to April 2004. The precision and total error of a single HOCl profile with a vertical resolution of about 9 km are approximately 0.05–0.08 ppbv and 0.05–0.09 ppbv, respectively (von Clarmann et al., 2006).

The Atmospheric Chemistry Experiment Fourier Transform Spectrometer (ACE-FTS) was launched on board the Canadian SCISAT satellite in 2003. The SCISAT low altitude (650 km), high inclination (74°) circular orbit allows a coverage of polar to tropical regions. The ACE-FTS instrument has a spectral resolution of 0.02 cm^{-1} from 750–4400 cm^{-1} and a vertical resolution of 3–4 km from the cloud tops to 150 km. The instrument collects infrared solar spectra from 15 sunrise and sunset occultations per

ACPD
12, 21065–21104, 2012

day (Bernath et al., 2005; Mahieu et al., 2008). The HCl data from the level 2 product of version 2.2 from November 2009 to April 2010 in the tropics are used in this study. To filter out the outliers present in this version of ACE-FTS data, the monthly median instead of the mean is used in each solar zenith angle bin.

3 Model and simulations

MISU-1D is a 1-D photochemical box model incorporating detailed radiative transfer calculations in the UV and visible region and state of the art stratospheric chemistry (Jonsson, 2006). Multiple scattering and albedo effects are treated according to Meier et al. (1982). The sphericity of the earth is taken into account which allows for non-zero transmitted flux at solar zenith angles greater than 90 degrees. The Earth-Sun distance is corrected for seasonal variations according to Madronich (1993). The variability in the solar flux over the 11-yr solar cycle is not considered in this study. The model includes a total of 120 reactions, constituting the most important gas-phase reactions in the stratosphere and mesosphere. The kinetic parameters for the calculation of rate constants and photolysis rates are mostly specified according to JPL 2006 recommendations, except for the reactions involving HOCl, HO_2 and HCl, which have been updated to JPL 2011 (Sander et al., 2011), and the rate of Reaction (R1), which is specified according to Stimpfle et al. (1979). The input solar flux for the calculation of photolysis rates is adopted from the World Meteorological Organization (WMO) reference spectrum. Ozone absorption cross sections and the oxygen absorption cross sections in the Schumann-Runge bands are in accordance with World Meteorological Organization (WMO) recommendations and the Koppers and Murtagh (1996) algorithm, respectively. The Herzberg continuum is taken from Nicolet and Kennes (1986).

Temperature and pressure for the simulated period November 2009 to April 2010 are taken from European Center for Medium-Range Weather Forecasts (ECMWF) analyses. The concentration of gases in the model is initialized with output from the Canadian Middle Atmosphere Model (CMAM). Short-lived species (e.g., radicals) are initialized

ACPD
12, 21065–21104, 2012

with zero concentrations and are generated by the chemical reactions in the model. Total inorganic chlorine, Cl_y, is constrained according to ACE-FTS observations in 2004 from 30° N to 30° S and altitudes 10 to 60 km (Nassar et al., 2006). Water vapor is initialized according to MLS observations (version 3.3) from November 2009 to April 2010 and between 20° N to 20° S. Figure 1 shows vertical profiles of chlorine and hydrogen species in the model at noon and midnight for solar conditions of 1 November at the equator. HCl is clearly the largest contributor to Cl_y, with secondary contributions from ClO, HOCl and $ClONO_2$ in the lower and middle stratosphere and from ClO and HOCl in the upper stratosphere and lower mesosphere. H_2O and H_2 are the main contributors to hydrogen family in all altitudes. The secondary contributors are OH and HO_2 from 35 to 55 km. Between 25 and 35 km, H_2O_2 dominates HO_x ([OH]+[HO_2]+[H]). The model is initialized for a specified time and location (latitude-longitude point) after which simulations can be performed either with a fixed or variable solar position. Here we perform diurnal cycles considering a variable sun position to generate day-night cycles. The model then runs for at least 40 days and the diurnal cycles of species concentrations change insignificantly between subsequent days. During the simulations, photolysis rates are extracted from a look-up table which is recalculated every 24 h using ozone concentrations calculated by the model. The reaction rate constants are calculated separately for each reaction depending on the temperature and are saved in a matrix for further use in differential equations. The chemical module solves a system of stiff ordinary differential equations with a variable order method according to Shampine and Reichelt (1997). This algorithm solves the time evolution of each species present in the reaction scheme (Jonsson, 2006).

The model has been applied for conditions of the times and locations of the SMILES measurements. This means that the length of the day and sunrise/sunset changes in the model correspond to the latitudes and seasonal effects in the measurements. We calculate the temporal development of HOCl, ClO, HO_2 and HCl at 35, 45 and 55 km for the latitudes 20° S, 0° and 20° N and for the first day of each month in the time period from November to April. Figure 2 shows the diurnal variation of the chlorine

ACPD
12, 21065–21104, 2012

and hydrogen species for solar conditions of 1 November at the equator. The diurnal variations are further discussed in Sect. 4.2.

4 Results and discussion

4.1 Observations

Figures 3 and 4 compare the diurnal variation of HOCl and the related species, ClO, HO_2 and HCl in observations from SMILES MLS, SMR, MIPAS and ACE-FTS with the *MISU-1D* model simulations. Throughout this study the observation results are, unless otherwise noted, averaged between 20° S to 20° N and over the full-life time period of SMILES from November 2009 to April 2010. For ACE-FTS HCl, the median is used instead of the mean in each solar zenith angle bin. The error bars represent the standard error of the mean observation for each individual data point. SMILES is represented by two different datasets, namely SMILES-O and SMILES-R. SMR, MIPAS and MLS provide data in a limited range of solar zenith angles, corresponding to the ascending and descending nodes at the equator of the respective satellite. ACE-FTS observations are limited to sunrise and sunset occultations. HO_2 data from MLS are corrected for bias by taking into account day-night differences and assuming negligible HO_2 during nighttime according to MLS user's guide documentation (Livesey et al., 2011). HO_2 data from SMR are averaged over the period October 2003 to October 2004 and HOCl data from MIPAS are averaged from November 2003 to April 2004, as these data are not available for the period November 2009 to April 2010. Consequently, some deviations in HOCl from MIPAS and HO_2 from SMR may be attributed to the different observation periods. The variability of each group of measurements is shown as a vertical error bar representing the respective 1-σ standard deviation. Next, in order to remove the offset the different datasets and to investigate the amplitude of the diurnal variations, the mean of the nighttime or morning volume mixing ratios at the respective levels is subtracted from the observations at other solar zenith angles. For SMILES and the

ACPD
12, 21065–21104, 2012

model, the nighttime volume mixing ratios for the solar zenith angle range measured by MLS are subtracted from daytime volume mixing ratios. The data are then shifted to match the SMILES-R data in the same solar zenith angle range (night). The results are shown in Figs. 5 and 6. This method decreases the discrepancies between the different satellite measurements and the simulations arising from biases in the data sets.

For HOCl (first row of Fig. 3), the MLS and MIPAS measurements follow the diurnal cycle measured by SMILES quite well, i.e. the difference between ascending and descending nodes of the MLS and MIPAS data corresponds well with the results from SMILES observations at the corresponding solar zenith angles. However, there are some differences. The SMILES HOCl observations are measured in bands A and B. The SMILES operational product (SMILES-O) is retrieved from band A, while the research product (SMILES-R) is retrieved from both bands A and B (same spectral line but different radiometer settings). The designed frequency region of band B is 625.12–626.32 GHz. In fact, the measured frequency region is wider than the nominal one and HOCl was observed at the edge of band B. Here, we compare the two bands for SMILES-R, although HOCl band B is on the border and its quality is expected to be less than band A. Despite some differences between band A and B from SMILES-R at 35 km, results from the two bands agree well at higher altitudes. The absolute HOCl values from MLS and MIPAS reside in the range of SMILES observation in the middle stratosphere, at 35 km. At this altitude, however, MIPAS measures similar HOCl values as SMILES-R band A (the maximum of the SMILES range) and MLS measures closer HOCl values to SMILES-R band B and SMILES-O (the minimum of the SMILES range). In the upper stratosphere at 45 km, MLS and all SMILES data sets agree well in terms of the absolute values, with the mean of MLS being in the range of the SMILES observations. MIPAS HOCl measurements are about 0.04 ppbv greater than the other observations at this altitude. The difference between the MIPAS data set and the other observations at these three altitudes should at least in part be due to the earlier time period of the MIPAS observations (using data from 2003/2004 as opposed to 2009/2010), as total inorganic chlorine (Cl_y) has been decreasing from about

ACPD
12, 21065–21104, 2012

year 2000 ownwards at this altitude (World Meteorological Organization (WMO), 2010). Additionally, due to the solar maximum activity in 2003/2004 compared to 2009/2010 (solar minimum), more OH production is expected (Wang et al., 2012). The enhanced OH leads to higher HO_2 and may have consequently increased the formation of HOCl by Reaction (R1). The daytime MLS observations at 45 km are more variable than those of MIPAS and SMILES showing a variability of 0.02 ppbv (1-σ standard deviation) at solar zenith angles ranging from 25° to 49°. In the lower mesosphere at 55 km, the MIPAS and SMILES HOCl mixing ratios show good agreement and the mean of differences does not exceed 0.007 ppbv. The MLS HOCl is not available at this altitude. In the first row of Fig. 5, the satellite observations of HOCl have been compared after offset correction to match the SMILES data. The amplitudes of the HOCl diurnal cycle deduced from MLS, SMILES, and MIPAS agree reasonably well at 35 and 45 km (the mean differences do not exceed 0.01 and 0.02 ppbv, respectively), however at 55 km the MIPAS diurnal cycle amplitude is about 0.02 ppbv smaller than that of SMILES.

ClO measurements by SMILES, MLS and SMR are presented in the second row of Fig. 3. At 35 km, the absolute values of ClO in volume mixing ratio agree quite well, however there are some minor differences. The mean of nighttime and the mean of daytime MLS are about 0.01 ppbv lower and 0.01 ppbv higher than corresponding SMILES observations, respectively. At 45 km, the SMR and SMILES (SMILES-R and SMILES-O) data agree reasonably well within about 0.01 ppbv. At the same altitude, MLS daytime measurements vary significantly compared with SMILES measurements within the range of solar zenith angles from 20 to 50°. The daytime ClO from MLS varies by about 0.05 ppbv (1-σ standard deviation) from its mean value (0.27 ppbv). At this altitude, the mean of MLS nighttime and daytime observations are higher than corresponding SMILES measurements by almost 0.04 and 0.05 ppbv, respectively. In the lower mesosphere at 55 km, SMILES-R ClO data are about 0.01 ppbv higher than SMILES-O data at all solar zenith angles. Both SMILES ClO data sets at this level show more ClO than sunrise and sunset observations by SMR (~ 0.035 ppbv). In the second row of Fig. 5, the offset corrected observations are shown. The amplitudes of

ACPD
12, 21065–21104, 2012

the observed diurnal variations agree reasonably at all altitudes (the absolute mean of differences does not exceed 0.06 ppbv), however there are some dissimilarities. At 35 km, the MLS amplitude is slightly larger (~ 0.01 ppbv) than the SMILES amplitude. The amplitude of SMR data at 45 km is about 0.03 ppbv larger than that of SMILES and about 0.06 ppbv smaller at 55 km.

The first row of Fig. 4 shows the HO_2 observed by MLS, SMILES and SMR at three altitudes. HO_2 measured by SMILES, SMR and MLS compares relatively well at all the altitudes of interest, particularly at 35 and 45 km, which the mean of differences is within the range of 0.01–0.025 ppbv, respectively. At 35 km, in spite of the variability of the SMR HO_2 measurements around the solar zenith angle of −90°, the mean of SMR data agrees quite well with both SMILES bands (mean of differences is about 0.01 ppbv). Despite of low quality of the SMILES-R band B compared to band C, we have chosen both bands for comparison in order to evaluate the measurements against each other. At this level, the results from SMILES-R and SMILES-O band B have both negative values at nighttime. As mentioned in the first paragraph of this section, MLS HO_2 measurements have been corrected for instrumental bias by taking into account the night-day differences. Due to the sun's maximum activity, when SMR data were collected (year 2003/2004) compared with the solar minimum activity (year 2009/2010) when other observations were made, SMR observes consistently the highest mixing ratios. Note also that SMR is not zero corrected for night-time HO_2 measurements as MLS, thus a bias cannot be completely excluded. The source of the HO_x family, in fact, is the photo-dissociation reactions generated by solar irradiance. At 45 km, the daytime HO_2 products of SMILES are in the range of about 0.28–0.35 ppbv. At this altitude, the results from MLS measurement of HO_2 (after bias correction) agree well with the results from SMILES range of measurements. HO_2 measured by SMR compares reasonably with SMILES observations of both bands and the mean of residuals are about 0.025 ppbv around the solar zenith angle of 90°. In the lower mesosphere at 55 km, SMILES-R and SMILES-O data at this level cover the range of about 0.46–0.55 ppbv at their maximum peak around noon. At this altitude, the mean of nighttime and daytime

ACPD
12, 21065–21104, 2012

MLS (about zero and 0.45 ppbv, respectively) are about 0.1 and 0.06 ppbv lower than that of the corresponding SMILES range of observations. The mean of sunrise SMR observations (about 0.16 ppbv) compares well with the SMILES range of observations, however, the SMR sunset observations (mean of about 0.37 ppbv) are about 0.05 ppbv larger at 55 km. In the first row of Fig. 6, the HO_2 amplitude (the difference of day and night) of the measurements agree well at 35 and 45 km. The amplitide of HO_2 observations by SMR and MLS at 55 km are about 0.15 and 0.05 ppbv larger than that of SMILES, respectively.

In the bottom row of Fig. 4, we show the HCl observations made by MLS, SMILES and ACE-FTS at 35, 45 and 55 km. There are some discrepancies between the different satellite observations of HCl in terms of the absolute values at all the altitudes of interest. As can be inferred from Figure 4, SMILES agrees with the mean of MLS and ACE-FTS observations within the range of 0.1–0.25 ppbv at 35 km, but it measures the lowest HCl among the observations at 45 and 55 km. The MLS and ACE-FTS data agree well at 45 km and the differences do not exceed 0.05 ppbv. The offset corrected measurements respective to SMILES, shown in the last row of Fig. 6, indicate that all observations show a very small HCl diurnal cycle. There are small differences between the diurnal cycle amplitude measured by SMILES, MLS and ACE-FTS. ACE-FTS and MLS data have slightly larger diurnal cycle amplitudes than the SMILES data at 45 and 55 km, however the differences do not exceed 0.1 ppbv. The ACE-FTS number of measurements at the tropics is small compared to the other instruments. This could cause more variation in the data due to the lower seasonal effect and statistical error.

4.2 Model comparison

Figures 3 and 4 show the model calculation of HOCl, ClO, HO_2 and HCl in gray shades. The observations shown in the Figure have already been discussed in the previous section. The model simulations have been carried out for the three latitudes (20° S, 0° and 20° N) and six representative months (November to April). To account for the different vertical resolution of the model and instruments, the model results have been

ACPD
12, 21065–21104, 2012

smoothed using a 5 km moving average for the 35 km level and a 7 km moving average for the 45 and 55 km panels. Model calculations have been shifted in Figures 5 and 6 to match SMILES observations at nighttime along with the other satellite data to investigate the reaction kinetics and the magnitude of the diurnal variation of the species in the model. The diurnal cycle amplitude depends on the initialization (e.g. Cl_y and H_2O) of the model, while the shape of the diurnal variation depends on reaction rate coefficients and photolysis parameters.

The diurnal variation of HOCl (first row of Fig. 2) exhibits very different patterns depending on the altitude. The peak of HOCl appears around noontime at 35 km and production dominates the loss by photolysis about 3 h after sunrise, in contrast to higher altitudes where the peak occurs at nighttime. At 35 km, HOCl formation by Reaction (R1) follows the HO_2 and ClO variations. Photolysis becomes more important at higher altitudes, resulting in a decrease of daytime HOCl. Moreover, due to the higher mixing ratio of HO_2 at higher altitudes, HOCl constantly forms at these altitudes but is photolysed easily. At 45 and 55 km, HOCl drops rapidly at sunrise, has more stabilized minimum concentrations during the course of the day and rises slowly after sunset. At the altitude of 45 km, HOCl is mostly governed by the ClO diurnal cycle. That can be confirmed by the anti-correlation of ClO and HOCl at this altitude. In the mesosphere (altitudes above 55 km), HOCl becomes a nocturnal sink for ClO after sunset due to the reaction of HO_2 and ClO.

As can be inferred from the first row of Fig. 3, the model reproduces a very similar shape of the diurnal variation of HOCl as the measurements at the three altitude levels. At 35 km, the model simulations match night observations by MIPAS and the SMILES-R range of observations and the differences are less than about 0.02 ppbv. The MLS observations are about 0.02 ppbv lower than the simulations. At 45 km, the model HOCl calculations match very well with the SMILES range of observations and MLS at nighttime and daytime, however daytime MLS data are rather scattered but the mean value agrees well with the model result and the differences do not exceed 0.01 ppbv. At this level, MIPAS measures about 0.05 ppbv more HOCl than the model

ACPD
12, 21065–21104, 2012

average at the corresponding solar zenith angles, as described earlier. The model and the observations agree quantitatively well at 55 km with the mean of differences being about 0.015 ppbv. The offset shifted model (respective to SMILES-R band B) is depicted in the first row of Fig. 5. The amplitude of the HOCl diurnal cycle deduced from the model and observations agree reasonably well within the range of 0.005–0.015 ppbv at all the altitudes, except for the MIPAS amplitude at 55 km which is about 0.02 ppbv smaller than that of the model and SMILES.

At 35 km, ClO rises sharply at sunrise and has a flat, fairly extended peak during daytime followed by a sharp drop after sunset in the middle stratosphere (see the first row of Fig. 2). The maximum peak of ClO in daytime at this altitude is mainly attributed to the photo-dissociation of $ClONO_2$. The dominant sink of nocturnal ClO is the combination of ClO and NO_2 and formation of $ClONO_2$ (Ko and Sze, 1984; Ricaud et al., 2000). At 45 and 55 km, the ClO diurnal variation is not just governed by HOCl and $ClONO_2$ (as $ClONO_2$ becomes less important with altitude), but is also influenced by odd oxygen chemistry ($O_x = O + O_3$). ClO at these altitudes and higher can react with free oxygen atoms and be converted to Cl atoms, leading to a ClO minimum during daytime.

The modelled diurnal variation of ClO at the three altitudes 35, 45 and 55 km is depicted in the bottom row of Fig. 3. ClO simulations generally reproduce very similar shapes as the observations at the altitudes of interest. The absolute values of simulations agree well with the MLS observations with differences being smaller then 0.01 ppbv at 35 km, and are slightly (~ 0.04 ppbv) higher than the daytime SMILES observations. The SMR mean of observations is about 0.05 ppbv lower than that of the simulations. At 45 km, the model reproduces a very similar daytime decrease of ClO consistently with the SMILES observations, as the result of reaction with free oxygen which converts part of ClO to atomic chlorine. The daytime chlorine increase can be seen in the second plot of the first row in Fig. 2. The SMILES observations of ClO at this altitude are about 0.1 ppbv lower than the model result and the mean of the MLS observations. Although the MLS daytime observation are fairly variable at 45 km (~ 0.05 ppbv

ACPD
12, 21065–21104, 2012

in terms of 1-σ standard deviation), the mean MLS values agree reasonably well with the model. At this altitude, SMR measures after sunset about 0.05 ppbv (~ 18 %) higher ClO mixing ratios than the simulations. At 55 km, the daytime and nighttime model calculations are about 0.02–0.04 ppbv higher than the SMILES range of observations. SMR also measures about 0.04–0.06 ppbv lower ClO than the model at 55 km. The comparison of the model diurnal cycle amplitudes of ClO, presented in the second row of Fig. 5, shows very similar amplitudes of the model and MLS at 35 and 45 km. The model amplitude of the diurnal variation agrees with that of SMR at 35 km, but is about 0.02 ppbv smaller and about 0.05 ppbv larger than that of SMR at 45 and 55 km, respectively. The model amplitude agrees with that of the two SMILES datasets at 45 km and the mean of differences does not exceed 0.01 ppbv, however it is about 0.04 ppbv and 0.02 ppbv larger than that of SMILES at 35 and 45 km, respectively.

The diurnal variation of HO_2 exhibits a very similar pattern from the middle stratosphere to the lower mesosphere. Very low values at nighttime and a sharp rise after sunrise which leads to the peak of HO_2 during the day, indicates the photolysis dependency of HO_2 formation (second row in Fig. 2). The rise of daytime HO_2 is mainly attributed to the reactions of H_2O with $O(^1D)$ in the stratosphere and lower mesosphere, where $O(^1D)$ is a product of ozone photolysis. The daytime mixing ratio increases with height, due to the more abundant atomic oxygen ($O(^1D)$) at higher altitudes. In Fig. 2, HO_x is the sum of OH, HO_2 and H. Methane oxidation is the other source of HO_2 formation. Since OH and HO_2 are tightly coupled through fast photochemical reactions, the source and sink of these molecules are the same. The drop after sunset is mainly due to the reaction of OH with NO_2 or HNO_3. The self reaction of OH and HO_2 is the other sink for both, producing water. The very small transient dip in the model HO_2 mixing ratios at dawn and dusk at 55 km can be observed in the SMILES measurements as well. Before sunrise, the small drop of mixing ratio is due to the reaction of HO_2 and atomic oxygen (which is generated by ozone photolysis). After sunset, the small transient decrease of HO_2 is because of the stop of the reaction of HO_2 with atomic oxygen, then HO_2 is produced by ozone and OH in a much lower rate.

ACPD
12, 21065–21104, 2012

HO_2 model simulations generally behave similarly as the observations and reproduce a very similar shape at all altitudes of interest, according to Fig. 4. At 35 km, the model result agrees reasonably well with the observations and the differences are below 0.01 ppbv. The nighttime model calculation of HO_2, the nighttime observations and the SMR observations agree well at 45 km and the differences do not exceed 0.01 ppbv, however the modelled daytime HO_2 is slightly lower than the average of the SMILES and MLS data by about 0.03 ppbv. At the altitude of 55 km, the daytime model calculations reside in the range of the SMILES observations, but give about 0.06 ppbv lower HO_2 than the daytime MLS observations. Although the SMR observations around sunrise are very close to the model, the observations after sunset are about 0.08 ppbv above the model average. The amplitude of the HO_2 diurnal variation has been compared with the amplitude from satellite data in the first row of Fig. 6. There is a good agreement between the observed HO_2 amplitudes and the model at 35 km and the mean of differences does not exceed 0.025 ppbv, but the model amplitude is about 0.03 ppbv (~ 11 %) smaller than the observations at 45 km. At 55 km, the model amplitude agrees well with that of SMILES (differences about 0.005 ppbv), however it is about 0.05 ppbv (~ 12 %) and 0.1 ppbv (~ 18 %) smaller than that of MLS and SMR, respectively.

HCl is the main chlorine reservoir in the stratosphere and mesosphere (see the plots in the first row of Fig. 2). HCl has only a weak diurnal variation in the middle and upper stratosphere, but increases slightly during the course of the day in the lower mesosphere. This diurnal variation cannot be seen in Fig. 2, but it is slightly better visualized in Figs. 4 and 6. This can be explained by the increased probability of the reaction of atomic chlorine with HO_2 which generates HCl during daytime, owing to the more abundant chlorine atoms and HO_2 radicals at this level.

Initializing the model with a realistic HCl profile as the main chlorine reservoir is crucial to get a correct amount of HOCl and ClO in the model. Here, we constrained the model with the total inorganic chlorine estimated from ACE-FTS observations between 30° S to 30° N and from 10 to 60 km according to Nassar et al. (2006) (Fig. 1). Although

ACPD
12, 21065–21104, 2012

reproducing a similar shape, the model simulations give higher HCl values compared with SMILES, MLS and ACE-FTS at all altitudes of interest, as can be inferred from the last row of Fig. 4. The model agrees better with the MLS and ACE-FTS data than with the SMILES observations in terms of the absolute HCl at all altitudes and the differences increase with height. Past trend studies have shown a decrease in the HCl concentration in the stratosphere and mesosphere (Froidevaux et al., 2006; World Meteorological Organization (WMO), 2010; Jones et al., 2011). Jones et al. (2011) analysis of HCl time series between 35 and 45 km at the tropics shows a linear trend of -5.8 ± 1.7 percent/decade. If the modelled HCl is corrected using Jones et al.'s (2011) estimation, then the HCl level at 35 and 45 km will be about 2.58 and 3.25 ppbv, respectively. Taking into account this correction, the model reproduces very close HCl volume mixing ratio to all observations at 35 km and to MLS and ACE-FTS at 45 km. If the model HCl is corrected with the trend rate of -0.78 ± 0.08 percent/year at 55 km estimated by Froidevaux et al. (2006), the model HCl would be about 3.5 ppbv and would match perfectly with MLS. The bottom row in Fig. 6 shows the offset shifted model and observations. The SMILES amplitude of HCl diurnal cycle, despite the differences in absolute values with the model at 45 and 55 km, agrees well with that of the model at these altitudes. MLS amplitude agrees best with that of the model at 55 km (the mean of differences does not exceed 0.005 ppbv), but there are some differences (about 3.5–0.6 %) at 35 and 45 km. The ACE-FTS amplitudes of diurnal cycle at 35 and 45 km are in the range of 0.4–3.5 % larger than the model and the SMILES amplitudes. It should be noted that some differences in the model and the observations could be due to the fact that the seasonal variability (e.g., transport) is not taken into account in the model calculation. Since we average the field observations over several months for a broad latitude bin, temporal and spatial changes within these bins over time and space can lead to variability in the measured data. The model cannot take care of such variabilities and just takes the temporal solar zenith angle variations into account.

ACPD
12, 21065–21104, 2012

4.3 Kinetics study

In this section, the sensitivity of the modelled HOCl to different reaction rates, k_1, for Reaction (R1) is investigated. k_1 is calculated according to Stimpfle et al. (1979), Nickolaisen et al. (2000), Hickson et al. (2007) as well as JPL 2006 and 2011 recommendations (Sander et al., 2011, 2006). The recommended value for calculation of k_1 in JPL 2011 is based on studies by Hickson et al. (2007), Nickolaisen et al. (2000), Knight et al. (2000) and Stimpfle et al. (1979) that studied Reaction (R1) as a function of temperature. Due to the clear day-night difference of mesospheric HOCl, observations above 40 km are well suited for testing the interactions between chlorine and hydrogen species. For this analysis, we carried out the simulations for 1 November at latitude 0°, which gives almost the average model calculations for the period and location of our study. The result has been compared with SMILES (SMILES-O and SMILES-R band A), MLS and MIPAS observations and is presented in the first row of Fig. 7 for 35, 45 and 55 km. In the second row of Fig. 7, the nighttime measurements and model concentrations are subtracted from the corresponding measurements and model and shifted respective to SMILES-R band B. The errors of the measurements are not plotted for better visualization of the model simulations in each case. The upper and lower uncertainty limit of k_1 according to JPL 2011 recommendations are also shown in the Figure. As can be inferred from the first row of the Figure, the best agreement between the model and the observations is achieved when using Nickolaisen et al. (2000) and Stimpfle et al. (1979) reaction rate equations, whilst using JPL 2006 and the lower and upper limits of JPL 2011 rate coefficient give the poorest agreement. This result confirms the study of rate constant, k_1, by Kovalenko et al. (2007) which has been done for lower altitudes (below 36 km). The reaction rate coefficients suggested by Hickson et al. (2007) and JPL 2011 also give HOCl in the range of the JPL 2011 uncertainty limits and the observations. The dissimilarities in HOCl levels between different k_1 decrease at higher altitudes and particularly during daytime. These results are confirmed when comparing the shifted observations and model runs (second row of Fig. 7). JPL 2006

ACPD
12, 21065–21104, 2012

and the lower limit of JPL 2011 give the lowest day-night amplitude at all altitudes. JPL 2011 recommendations give smaller day-night amplitude than the observations, Stimpfle et al. (1979) and Nickolaisen et al. (2000) reaction rate constants. According to the first row of the figure, the modelled HOCl is mostly sensitive to k_1 during night-time at all altitudes of interest. It is also sensitive to k_1 during daytime at 35 and 45 km. The effect of various k_1 is negligible on the modelled ClO and HO_2.

5 Summary and conclusions

The diurnal variations of HOCl, ClO, HO_2 and HCl calculated with a 1-D chemical model were compared with observations of these species by three sub-millimeter instruments (Odin/SMR, AURA/MLS and SMILES) and two infrared spectrometers (SCISAT/ACE-FTS and ENVISAT/MIPAS) for the period of SMILES operations from November 2009 to April 2010, the latitude range of 20° N to 20° S, and three levels from the middle stratosphere to the lower mesosphere. SMILES data and the model results are available for the whole range of solar zenith angles and thus allow to compare indirectly the MLS, SMR, MIPAS and ACE-FTS observations of the short-lived species. This analysis includes new SMILES data, a new version of HO_2 measured by SMR and the latest version of MLS data.

The satellite observations of HOCl, ClO, HO_2 and HCl diurnal variations generally agree well both in quantity and in shape, considering the difficulties of comparisons between sun-synchronous and solar occultation instruments. The modelled species generally reproduce very similar shapes of the diurnal variation as obtained from the satellite observations in the tropics at the altitudes 35, 45 and 55 km, where HOCl is mainly formed by the reaction of ClO and HO_2. The differences between the day and night data from model and satellites indicate almost similar diurnal variation amplitudes of the modelled and observed species.

The absolute values of HOCl (in volume mixing ratio) from the simulations, MIPAS and MLS agree with the range of SMILES observations at 35 km. The model and the

ACPD
12, 21065–21104, 2012

observations agree well at 45 and 55 km, however MIPAS measures about three times higher HOCl at 45 km. Better agreement cannot be expected as the MIPAS data are taken from November 2003 to April 2004, when overall chlorine level was higher. The difference between the day and night data from the model and satellites, showing the amplitude of the diurnal variation, indicate a very similar amplitude for the MLS, MIPAS and SMILES data as well as that of the model result at 35 and 45 km, but a slightly smaller amplitude for the MIPAS data compared with the model and the other instruments at 55 km.

The model ClO agrees well in absolute volume mixing ratio values with the observations at 35 and 55 km, however it calculates slightly higher daytime ClO than the SMILES measurements. The model is also slightly higher than nighttime SMILES and SMR observations at their respective solar angles at 55 km. After offset shift, the model amplitude of ClO between night and day agrees reasonably with that of the MLS and SMR data at 35 and 45 km, but it is larger than that of SMR at 55 km. The SMILES amplitude of the ClO diurnal cycle agree with that of the model at 45 km, but is slightly smaller at 35 and 45 km.

Odin/SMR HO_2 data has not been compared previously with other satellite observations and this study represents the first validation of SMR HO_2. Although SMR HO_2 have been taken from a different time period than the other satellite observations, and despite the different solar activity during respective periods of observation, there is generally a good agreement between the SMR, MLS and SMILES observations and the simulations. Nevertheless, the SMR data after sunset are slightly higher than the model and the SMILES data at all altitudes. The absolute values of HO_2 agree best at 35 km, but the differences between the model and the observations are slightly larger at 45 and 55 km. At 45 km, MLS and all SMILES data sets agree and are slightly higher than the model simulations. At 55 km, the model daytime calculations and the observations agree well, but there are some differences in nighttime and sunset observations by MLS, SMR and SMILES compared to the model. After offset correction, very similar amplitudes of the observations and the model are obtained for the 35 km level. The

ACPD
12, 21065–21104, 2012

amplitude of all observations are slightly larger than that of the model at 45 km. The SMILES and the model amplitudes agree well at 55 km and are smaller than that of MLS and SMR.

The model and observations show a very weak diurnal variation of HCl at the three altitudes of 35, 45 and 55 km. There is a reasonable agreement between the observations at 35 km, but the MLS and ACE-FTS measurements are higher than the SMILES data at 45 and 55 km. The model calculates higher HCl than the SMILES data, closer to the ACE-FTS and MLS data particularly at 45 and 55 km. This can be explained as the model is initialized with the Cl_y profile measured by ACE-FTS (Nassar et al., 2006). The model result is consistent with the MLS and ACE-FTS data when HCl trend estimations by Froidevaux et al. (2006) and Jones et al. (2011) are considered.

The reaction rate coefficients of HOCl formation (k_1) by Stimpfle et al. (1979) and Nickolaisen et al. (2000), Hickson et al. (2007) and JPL 2011 recommendations (Sander et al., 2011) provide a reasonably good agreement between the model and observations. All reaction rates studied here reside in the range of upper and lower uncertainty limits of JPL 2011. JPL 2006 and the upper and lower uncertainty limits of the JPL 2011 recommendations for k_1 give the worst agreement with the model and the observations. This result confirms the study by Kovalenko et al. (2007) which was done for lower altitudes (below 36 km). In case of using the JPL 2011, the night-day differences of HOCl volume mixing ratios underestimate that of the observations. This analysis confirms that gas phase chemistry of the reaction $HO_2 + ClO$ based on latest recommendations of k_1 is rather well understood.

The general good agreement of the model and observed diurnal cycles can be used in the future to correct long-term datasets differing in local time using scaling factor from model simulations to obtain realistic time series for trend analysis (e.g., Brohede et al., 2007; Jones et al., 2011).

Acknowledgements. The retrievals of IMK/IAA were performed on the HP XC4000 of the Scientific Supercomputing Center (SSC) Karlsruhe under project grant MIPAS. IMK data analysis was supported by DLR under contract number 50EE0901. MIPAS level 1B data were provided by

ACPD
12, 21065–21104, 2012

ESA. Odin is a Swedish-led satellite project funded jointly by Sweden (SNSB), Canada (CSA), Finland (TEKES), and France (CNES). Since 2007 the Odin project is supported by the third party mission programme of the European Space Agency (ESA). The JEM/SMILES mission is a joint project of the Japan Aerospace Exploration Agency (JAXA) and the National Institute of Information and Communications Technology (NICT). Work at the Jet Propulsion Laboratory, California Institute of Technology, was done under contract with the National Aeronautics and Space Administration.

References

Abbatt, J. and Molina, M.: The heterogeneous reaction of HOCl + HCl → Cl_2 + H_2O on ice and nitric acid trihydrate: reaction probabilities and stratospheric implications, Geophys. Res. Lett., 19, 461–464, 1992. 21068

Baron, P., Dupuy, E., Urban, J., Murtagh, D., Eriksson, P., and Kasai, Y.: HO_2 measurements in the stratosphere and the mesosphere from the sub-millimetre limb sounder Odin/SMR, Int. J. Remote Sens., 30, 4195–4208, 2009. 21071

Baron, P., Urban, J., Sagawa, H., Möller, J., Murtagh, D. P., Mendrok, J., Dupuy, E., Sato, T. O., Ochiai, S., Suzuki, K., Manabe, T., Nishibori, T., Kikuchi, K., Sato, R., Takayanagi, M., Murayama, Y., Shiotani, M., and Kasai, Y.: The Level 2 research product algorithms for the Superconducting Submillimeter-Wave Limb-Emission Sounder (SMILES), Atmos. Meas. Tech., 4, 2105–2124, doi:10.5194/amt-4-2105-2011, 2011. 21072, 21073

Barret, B., Ricaud, P., Santee, M., Attie, J., Urban, J., Le Flochmoën, E., Berthet, G., Murtagh, D., Eriksson, P., Jones, A., De La Noë, J., Dupuy, E., Froideveaux, L., Livesey, N. J., Waters, J. W., and Filipiak, M. J.: Intercomparisons of trace gases profiles from the Odin/SMR and Aura/MLS limb sounders, J. Geophys. Res., 111, 21302, doi:10.1029/2006JD007305, 2006. 21071

Bernath, P. F., McElroy, C. T., Abrams, M. C., Boone, C. D., Butler, M., Camy-Peyret, C., Carleer, M., Clerbaux, C., Coheur, P.-F., Colin, R., De Cola, P., De Mazière, M., Drummond, J. R., Dufour, D., Evans, W. F. J., Fast, H., Fussen, D., Gilbert, K., Jennings, D. E., Llewellyn, E. J., Lowe, R. P., Mahieu, E., Mcconnell, J. C., McHugh, M., Mcleod, S. D., Michaud, R., Midwinter, C., Nassar, R., Nichitiu, F., Nowlan, C., Rinsland, C. P., Rochon, Y. J., Rowlands, N., Semeniuk, K., Simon, P., Skelton, R., Sloan, J. J., Soucy, M.-A., Strong, K., Tremblay,

ACPD

12, 21065–21104, 2012

P., Turnbull, D., Walker, K. A., Walkty, I., Wardle, D. A., Wehrle, V., Zander, R., and Zou, J.: Atmospheric Chemistry Experiment (ACE): Mission overview, Geophys. Res. Lett., 32, L15S01, doi:10.1029/2005GL022386, 2005. 21074

Brohede, S., McLinden, C., Berthet, G., Haley, C., Murtagh, D., and Sioris, C.: A stratospheric NO_2 climatology from Odin/OSIRIS limb-scatter measurements, Can. J. Phys., 85, 1253–1274, 2007. 21089

Burrows, J. and Cox, R.: Kinetics of chlorine oxide radical reactions using modulated photolysis. Part 4. The reactions Cl + Cl_2O → Cl_2 + ClO and ClO + HO_2 products studied at 1 atm and 300 K, J. Chem. Soc., Faraday Trans. 1, 2465–2479, 1981. 21068

Chance, K., Johnson, D., and Traub, W.: Measurement of stratospheric HOCl: Concentration profiles, including diurnal variation, J. Geophys. Res., 94, 11059–11069, doi:10.1029/JD094iD08p11059, 1989. 21068, 21069

Dupuy, E., Urban, J., Ricaud, P., Le Flochmoën, E., Lautié, N., Murtagh, D., De La Noë, J., El Amraoui, L., Eriksson, P., Forkman, P., Frisk, U., Jégou, F., Jiménez, C., and Olberg, M.: Strato-mesospheric measurements of carbon monoxide with the Odin Sub-Millimetre Radiometer: Retrieval and first results, Geophys. Res. Lett., 31, L20101, doi:10.1029/2004GL020558, 2004. 21071

Frisk, U., Hagström, M., Ala-Laurinaho, J., Andersson, S., Berges, J.-C., Chabaud, J.-P., Dahlgren, M., Emrich, A., Florén, H.-G., Florin, G., Fredrixon, M., Gaier, T., Haas, R., Hirvonen, T., Hjalmarsson, Å., Jakobsson, B., Jukkala, P., Kildal, P., Kollberg, E., Lassing, J., Lecacheux, A., Lehikoinen, P., Lehto, A., Mallat, J., Marty, C., Michet, D., Narbonne, J., Nexon, M., Olberg, M., Olofsson, O., Olofsson, G., Origné, A., Petersson, M., Piironen, P., Pons, R., Pouliquen, D., Ristocelli, I., Rosolen, C., Rouaix, G., Räisänen, A., Serra, G., Sjöberg, F., Stenmark, L., Torchinsky, S., Tuovinen, J., Ullberg, C., Vinterhav, E., Wadefalk, N., Zirath, H., Zimmermann, P., and Zimmermann, R.: The Odin satellite: I. Radiometer design and test, Astron. Astrophys., 402, L27–L34, 2003. 21071

Froidevaux, L., Livesey, N., Read, W., Salawitch, R., Waters, J., Drouin, B., MacKenzie, I., Pumphrey, H., Bernath, P., Boone, C., Nassar, R., Montzka, S., Elkins, J., Cunnold, D., and Waugh, D.: Temporal decrease in upper atmospheric chlorine, Geophys. Res. Lett., 33, L23812, doi:10.1029/2006GL027600, 2006. 21085, 21089

Froidevaux, L., Jiang, Y. B., Lambert, A., Livesey, J., Read, W. G., J. W. Waters, R. A. F., Marcy, T. P., Popp, P. J., Fahey, R. S. G. D. W., Jucks, K. W., Stachnik, R. A., Toon, G. C., Christensen, L. E., Webster, C. R., Bernath, P. F., Boone, C. D., Walker, K. A., Pumphrey, H. C., Harwood,

ACPD
12, 21065–21104, 2012

R. S., Manney, G. L., Schwartz, M. J., Daffer, W. H., Drouin, B. J., Cofield, R. E., Cuddy, D. T., Jarnot, R. F., Knosp, B. W., Perun, V. S., Snyder, W. V., Stek, P. C., Thurstans, R. P., and Wagner, P. A.: Validation of Aura Microwave Limb Sounder HCl measurements, J. Geophys. Res, 113, D15S25, doi:10.1029/2007JD009025, 2008. 21071

Hanson, D. and Ravishankara, A.: Investigation of the reactive and nonreactive processes involving $ClONO_2$ and HCl on water and nitric acid doped ice, J. Phys. Chem., 96, 2682–2691, 1992. 21068

Hickson, K., Keyser, L., and Sander, S.: Temperature dependence of the HO_2 + ClO reaction. 2. Reaction kinetics using the discharge-flow resonance-fluorescence technique, J. Phys. Chem. A, 111, 8126–8138, 2007. 21068, 21086, 21089, 21104

Johnson, D., Traub, W., Chance, K., Jucks, K., and Stachnik, R.: Estimating the abundance of ClO from simultaneous remote sensing measurements of HO_2, OH, and HOCl, Geophys. Res. Lett., 22, 1869–1871, 1995. 21069

Jones, A., Urban, J., Murtagh, D. P., Sanchez, C., Walker, K. A., Livesey, N. J., Froidevaux, L., and Santee, M. L.: Analysis of HCl and ClO time series in the upper stratosphere using satellite data sets, Atmos. Chem. Phys., 11, 5321–5333, doi:10.5194/acp-11-5321-2011, 2011. 21085, 21089

Jonsson, A.: Modelling the middle atmosphere and its sensitivity to climate change, Stockholm University, 2006. 21074, 21075

Jucks, K., Johnson, D., Chance, K., Traub, W., Margitan, J., Osterman, G., and Salawitch, R.: Observations of OH, HO_2, H_2O, and O_3 in the upper stratosphere: implications for photochemistry, Geophys. Res. Lett., 25, 3935–3938, 1998. 21070

Kasai, Y., Sagawa, H., Sato, T., Kuribayashi, K., Baron, P., and Mendrok, J.: The first observation of diurnal variation of HOCl by SMILE, Atmos. Chem. Phys. Discuss., in preparation, 2012. 21073

Kikuchi, K., Nishibori, T., Ochiai, S., Ozeki, H., Irimajiri, Y., Kasai, Y., Koike, M., Manabe, T., Mizukoshi, K., Murayama, Y., Nagahama, T., Sano, T., Sato, R., Seta, M., Takahashi, Ch., Takayanagi, M., Masuko, H., Inatani, J., Suzuki, M., and Shiotani, M.: Overview and early results of the Superconducting Submillimeter-Wave Limb-Emission Sounder (SMILES), J. Geophys. Res, 115, D23306, doi:10.1029/2010JD014379, 2010. 21069, 21072

Knight, G., Beiderhase, T., Helleis, F., Moortgat, G., and Crowley, J.: Reaction of HO_2 with ClO: Flow tube studies of kinetics and product formation between 215 and 298 K, J. Phys. Chem. A, 104, 1674–1685, 2000. 21068, 21086

ACPD
12, 21065–21104, 2012

Ko, M. and Sze, N.: Diurnal variation of ClO: Implications for the Stratospheric Chemistries of $ClONO_2$, HOCl, and HCl, J. Geophys. Res., 89, 11619–11632, doi:10.1029/JD089iD07p11619, 1984. 21082

Koppers, G. A. and Murtagh, D. P.: Model studies of the influence of O_2 photodissociation parametrizations in the Schumann-Runge bands on ozone related photolysis on the upper atmosphere, Annales Geophysicae, 14, 68–79, 1996. 21074

Kovalenko, L., Jucks, K., Salawitch, R., Toon, G., Blavier, J., Johnson, D., Kleinbohl, A., Livesey, N., Margitan, J., Pickett, H., Livesey, N. J., Margitan, J. J., Pickett, H. M., Santee, M. L., Sen, B., Stachnik, R. A., and Waters, J. W.: Observed and modeled HOCl profiles in the midlatitude stratosphere: Implication for ozone loss, Geophys. Res. Lett., 34, L19801, doi:10.1029/2007GL031100, 2007. 21068, 21086, 21089

Larsen, J., Rinsland, C., Goldman, A., Murcray, D., and Murcray, F.: Upper limits for stratospheric H_2O_2 and HOCl from high resolution balloon-borne infrared solar absorption spectra, Geophys. Res. Lett., 12, 663–666, 1985. 21069

Leck, T. J., Cook, J. E. L., and Birks, J. W.: Studies of reactions of importance in the stratosphere. III. Rate constant and products of the reaction between ClO and HO_2 radicals at 298 K, J. Chem. Phys., 72, 2364–2374, doi:10.1063/1.439484, 1980. 21068

Livesey, N., Read, W. G., Froidevaux, L., Lambert, A., Manney, G. L., Pumphrey, H. C., Santee, M. L., Schwartz, M. J., Wang, S., Eld, R. E. C., Cuddy, D. T., Fuller, R. A., Jarnot, R. F., Jiang, J. H., Knosp, B. W., Stek, P. C., Wagner, P. A., and Wu., D. L.: EOS MLS Level 2 Version 3.3 Quality Document, Tech. rep., Jet Propulsion Laboratory, California Institute of Technology, Pasadena, California, 91109-8099, http://mls.jpl.nasa.gov/data/datadocs.php, 2011. 21072, 21076

Madronich, S.: The atmosphere and UV-B radiation at ground level, in: Environmental UV Photobiology, edited by: Bjorn, L. O. and Young, A. R., 1993. 21074

Mahieu, E., Duchatelet, P., Demoulin, P., Walker, K. A., Dupuy, E., Froidevaux, L., Randall, C., Catoire, V., Strong, K., Boone, C. D., Bernath, P. F., Blavier, J.-F., Blumenstock, T., Coffey, M., De Mazière, M., Griffith, D., Hannigan, J., Hase, F., Jones, N., Jucks, K. W., Kagawa, A., Kasai, Y., Mebarki, Y., Mikuteit, S., Nassar, R., Notholt, J., Rinsland, C. P., Robert, C., Schrems, O., Senten, C., Smale, D., Taylor, J., Tétard, C., Toon, G. C., Warneke, T., Wood, S. W., Zander, R., and Servais, C.: Validation of ACE-FTS v2.2 measurements of HCl, HF, CCl3F and CCl2F2 using space-, balloon- and ground-based instrument observations, Atmos. Chem. Phys., 8, 6199–6221, doi:10.5194/acp-8-6199-2008, 2008. 21074

ACPD
12, 21065–21104, 2012

Meier, R. R., Anderson Jr., D. E., and Nicolet, M.: Radiation field in the troposphere and stratosphere from 240–1000 NM-I. General analysis, Planet. Space Sci., 30, 923–933, doi:10.1016/0032-0633(82)90134-9, 1982. 21074

Mitsuda, C., Suzuki, M., Iwata, Y., Manago, N., Naito, Y., Takahashi, C., Imai, K., Nishimoto, E., Hayashi, H., Shiotani, M., Sano, T., Takayanagi, M., and Taniguchi, H.: Current status of level 2 product of Superconducting Submillimeter-Wave Limb-Emission Sounder (SMILES), SPIE, 8176, 81760M, doi:10.1117/12.898135, 2011. 21072

Murtagh, D., Frisk, U., Merino, F., Ridal, M., Jonsson, A., Stegman, J., Witt, G., Eriksson, P., Jiménez, C., Mégie, G., de La Noë, J., Ricaud, P., Baron, P., Pardo, J., Hauchecorne, A., Llewellyn, E., Degenstein, D., Gattinger, R., Lloyd, N., Evans, W., McDade, I., Haley, C., Sioris, C., von Savigny, C., Solheim, B., McConnell, J., Strong, K., Richardson, E., Leppelmeier, G., Kyrölä, E., Auvinen, H., and Oikarinen, L.: An overview of the Odin atmospheric mission, Can. J. Phys., 80, 309–319, 2002. 21071

Nassar, R., Bernath, P., Boone, C., Clerbaux, C., Coheur, P., Dufour, G., Froidevaux, L., Mahieu, E., McConnell, J., McLeod, S., Murtagh, D. P., Rinsland, C. P., Semeniuk, K., Skelton, R., Walker, K. A., and Zander, R.: A global inventory of stratospheric chlorine in 2004, J. Geophys. Res, 111, D22312, doi:10.1029/2006JD007073, 2006. 21075, 21084, 21089, 21098

Nickolaisen, S., Roehl, C., Blakeley, L., Friedl, R., Joseph, S., Liu, R., and Sander, S.: Temperature Dependence of the HO_2 + ClO Reaction. 1. Reaction Kinetics by Pulsed Photolysis-Ultraviolet Absorption and ab Initio Studies of the Potential Surface, J. Phys. Chem. A, 104, 308–319, 2000. 21068, 21086, 21087, 21089, 21104

Nicolet, M. and Kennes, R.: Aeronomic problems of the moleculatr oxygen photodissociation I. The O_2 Herzberg continuum., Planet, 34, 1043, 1043–1059, doi:10.1016/0032-0633(86)90015-2, 1986. 21074

Pickett, H., Drouin, B., Canty, T., Salawitch, R., Fuller, R., Perun, V., Livesey, N., Waters, J., Stachnik, R., Sander, S., Traub, W. A., Jucks, K. W., and Minschwaner, K.: Validation of Aura Microwave limb sounder OH and HO_2 measurements, J. Geophys. Res, 113, D16S30, doi:10.1029/2007JD008775, 2008. 21071

Raper, O., Farmer, C., Zander, R., and Park, J.: Infrared spectroscopic measurements of halogenated sink and reservoir gases in the stratosphere from the ATMOS Spacelab 3 mission, J. Geophys. Res, 92, 9851–9858, 1987. 21069

Reimann, B. and Kaufman, F.: Rate constant of the reaction HO + ClO → HOCl + O, J. Chem. Phys., 69, 2925–2926, 1978. 21068

ACPD
12, 21065–21104, 2012

Ricaud, P., Chipperfield, M., Waters, J., Russell III, J., and Roche, A.: Temporal evolution of chlorine monoxide in the middle stratosphere, J. Geophys. Res., 105, 4459–4469, 2000. 21069, 21082

Sander, S., Friedl, R., Barker, J., Golden, D., Kurylo, M., Wine, P., Abbatt, J., Burkholder, J., Kolb, C., Moortgat, G., Huie, R. E., and Orkin, V. L.: Chemical kinetics and photochemical data for use in Atmospheric Studies Evaluation Number 17, Tech. rep., JPL, evaluation number 17, JPL Publ., 10-6, 2011. 21069, 21074, 21086, 21089, 21104

Sander, S. P., Friedl, R. R., Barker, J. R., Golden, D., Kurylo, M., Wine, P., Abbatt, J., Burkholder, J., Kolb, C., Moortgat, G., Huie, R. E., and Orkin, V. L.: Chemical kinetics and photochemical data for use in Atmospheric Studies Evaluation Number 15, Tech. rep., JPL, evaluation number 15, JPL Publ., 06-2, 2006. 21068, 21069, 21086

Santee, M., Lambert, A., Read, W., Livesey, N., Coeld, R., Cuddy, D., Daffer, W., Drouin, B., Froidevaux, L., Fuller, R., Jarnot, R., Knosp, B., Manney, G., Perun, V., Snyder, W., Stek, P., Thurstans, R., Wagner, P., Waters, J., Urban, J., Murtagh, D., Ricaud, P., Barret, B., Kleinböhl, A., Kuttippurath, J., Küllmann, H., Toon, G., and Stachnik, R.: Validation of the Aura Microwave Limb Sounder ClO Measurements, J. Geophys. Res., 113, 20 pp., doi:10.1029/2007JD008762, 2008. 21071

Sato, T. O., Sagawa, H., Kreyling, D., Manabe, T., Ochiai, S., Kikuchi, K., Baron, P., Mendrok, J., Urban, J., Murtagh, D., Yasui, M., and Kasai, Y.: Strato-mesospheric ClO observations by SMILES: error analysis and diurnal variation, Atmos. Meas. Tech. Discuss., 5, 4667–4710, doi:10.5194/amtd-5-4667-2012, 2012. 21069, 21072, 21073

Shampine, L. and Reichelt, M. W.: The Matlab ODE suite, SIAM J. Sci. Comput., 18, 1–22, 1997. 21075

Stimpfle, R. M., Perry, R. A., and Howard, C. J.: Temperature dependence of the reaction of ClO and HO_2 radicals, J. Chem. Phys., 71, 5183–5190, 1979. 21068, 21074, 21086, 21087, 21089, 21104

Takahashi, C., Ochiai, S., and Suzuki, M.: Operational retrieval algorithms for JEM/SMILES level 2 data processing system, J. Quant. Spectrosc. Ra., 111, 160–173, 2010. 21072

Takahashi, C., Suzuki, M., Mitsuda, C., Ochiai, S., Manago, N., Hayashi, H., Iwata, Y., Imai, K., Sano, T., Takayanagi, M., and Shiotani, M.: Capability for ozone high-precision retrieval on JEM/SMILES observation, Adv. Space Res., 48, 1076–1085, 2011. 21072

ACPD

12, 21065–21104, 2012

Toon, G., Farmer, C., Schaper, P., Lowes, L., and Norton, R.: Composition measurements of the 1989 Arctic winter stratosphere by airborne infrared solar absorption spectroscopy, J. Geophys. Res., 97, 7939–7961, 1992. 21069

Urban, J., Lautie, N., Flochmoën, E. L., Jimenez, C., Eriksson, P., de La Noë, J., Dupuy, E., Ekström, M., Amraoui, L. E., Frisk, U., Murtagh, D., Olberg, M., and Ricaud, P.: Odin/SMR limb observations of stratospheric trace gases: Level 2 processing of ClO, N_2O, HNO_3, and O_3, J. Geophys. Res, 110, D114307, doi:10.1029/2004JD005741, 2005. 21071

Urban, J., Murtagh, D., Lautié, N., Barret, B., Dupuy, E., de La Noë, J., Eriksson, P., Frisk, U., Jones, A., Le Flochmoën, E., Olberg, M., Piccolo, C., Ricaud, P., and Rösevall, J.: Odin/SMR Limb Observations of Trace Gases in the Polar Lower Stratosphere during 2004–2005, in: Proc. ESA First Atmospheric Science Conference, 8–12 May 2006, Frascati, Italy, edited by: Lacoste, H., vol. ESA-SP-628 of *European Space Agency publications*, European Space Agency, ISBN-92-9092-939-1, ISSN-1609-042X, 2006. 21071

von Clarmann, T., Wetzel, G., Oelhaf, H., Friedl-Vallon, F., Linden, A., Maucher, G., Seefeldner, M., Trieschmann, O., and Lefevre, F.: $ClONO_2$ vertical profile and estimated mixing ratios of ClO and HOCl in winter arctic stratosphere from Michelson interferometer for passive atmospheric sounding limb emission spectra, J. Geophys. Res., 102, 16157–16168, 1997. 21069

von Clarmann, T., Glatthor, N., Grabowski, U., Höpfner, M., Kellmann, S., Linden, A., Tsidu, G., Milz, M., Steck, T., Stiller, G., Fischer, H., and Funke, B.: Global stratospheric HOCl distributions retrieved from infrared limb emission spectra recorded by the Michelson Interferometer for Passive Atmospheric Sounding (MIPAS), J. Geophys. Res., 111, D05311, doi:10.1029/2005JD005939, 2006. 21069, 21073

von Clarmann, T., Glatthor, N., Ruhnke, R., Stiller, G. P., Kirner, O., Reddmann, T., Höpfner, M., Kellmann, S., Kouker, W., Linden, A., and Funke, B.: HOCl chemistry in the Antarctic Stratospheric Vortex 2002, as observed with the Michelson Interferometer for Passive Atmospheric Sounding (MIPAS), Atmos. Chem. Phys., 9, 1817–1829, doi:10.5194/acp-9-1817-2009, 2009. 21068, 21069

von Clarmann, T., Funke, B., Glatthor, N., Kellmann, S., Kiefer, M., Kirner, O., Sinnhuber, B.-M., and Stiller, G. P.: The MIPAS HOCl climatology, Atmos. Chem. Phys., 12, 1965–1977, doi:10.5194/acp-12-1965-2012, 2012. 21068

ACPD
12, 21065–21104, 2012

Wang, S., Li, K., Pongetti, T. J., Sander, S. P., Yung, Y. L., Liang, M., Livesey, N. J., Santee, M. L., Harder, J. W., Snow, M., and Mills, F. P.: Mid-latitude Atmospheric OH Response to the Most Recent 11-year Solar Cycle, P. Natl. Acad. Sci., submitted, 2012. 21078

Waters, J., Froidevaux, L., Harwood, R., Jarnot, R., Pickett, H., Read, W., Siegel, P., Cofield, R., Filipiak, M., Flower, D., Holden, J. R., Lau, G. K., Livesey, N. J., Manney, G. L., Pumphrey, H. C., Santee, M. L., Wu, D. L., Cuddy, D. T., Lay, R. R., Loo, M. S., Perun, V. S., Schwartz, M. J., Stek, P. C., Thurstans, R. P., Boyles, M. A., Chandra, K. M., Chavez, M. C., Chen, G.-S., Chudasama, B. V., Dodge, R., Fuller, R. A., Girard, M. A., Jiang, J. H., Jiang, Y., Knosp, B. W., LaBelle, R. C., Lam, J. C., Lee, K. A., Miller, D., Oswald, J. E., Patel, N. C., Pukala, D. M., Quintero, O., Scaff, D. M., Van Snyder, W., Tope, M. C., Wagner, P. A., and Walch, M. J.: The Earth Observing System Microwave Limb Sounder (EOS MLS) on the Aura satellite, IEEE T. Geosci. Remote Sens., 44, 1075–1092, 2006. 21069

World Meteorological Organization (WMO): Atmospheric Ozone 1985, WMO Global Ozone Research and Monitoring Project, Report No. 16, Geneva, 1986. 21074

World Meteorological Organization (WMO): Scientific Assesment of Ozone Depletion 2010, WMO Global Ozone Research and Monitoring Project, Report No. 52, Geneva, 2010. 21078, 21085

ACPD

12, 21065–21104, 2012

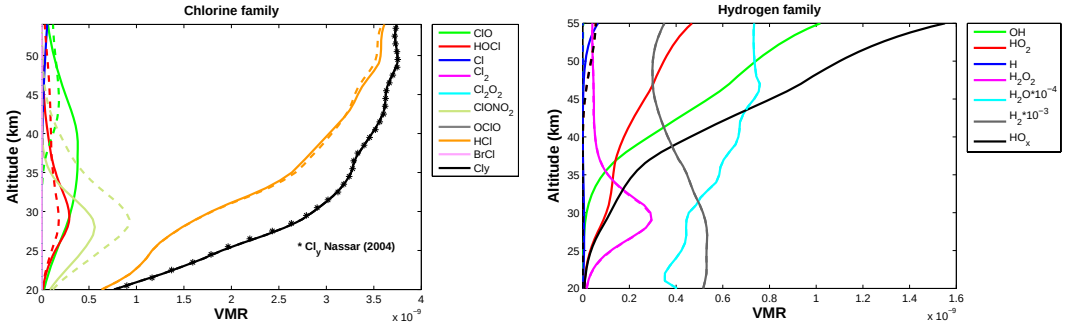

Fig. 1. Chlorine species profiles (on the left) and hydrogen species profiles (on the right) simulated for conditions of 1st November in the tropics. The total inorganic chlorine in the model is constrained according to measurements by ACE-FTS from 30° S to 30° N and altitudes 10 to 60 km (Nassar et al., 2006). Water is initialized according to water profiles measured by MLS on 1 November 2009. Temperature and pressure profiles are taken from ECMWF analyses for the same day. Profiles of the model species at noon are shown as solid lines and profiles at midnight as dashed lines.

ACPD
12, 21065–21104, 2012

HOCl, ClO and HO_2 diurnal variation in the tropics

M. Khosravi et al.

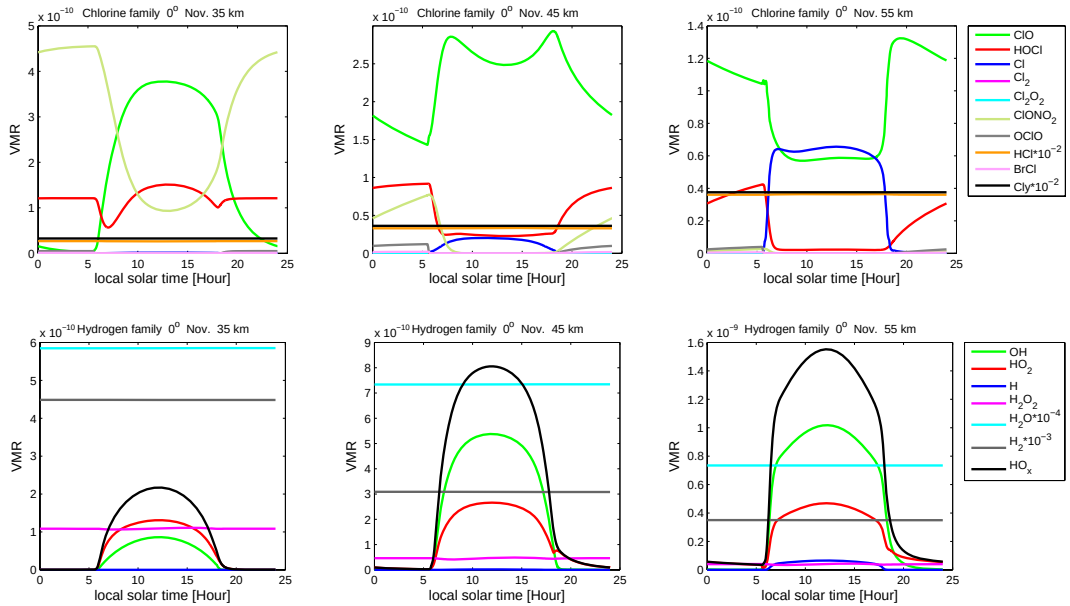

Fig. 2. Modeled diurnal variation of chlorine species (top row) and hydrogen species (bottom row) in the tropics (latitude 0°) calculated for November 1 and altitudes of 35, 45 and 55 km (left, middle and right). The diurnal variation of species are presented as volume mixing ratio versus local solar time. HCl and Cl_y (in the first row) and H_2O and H_2 (in the second row) have been scaled down for better visualization of minor species (see legend). HO_x is the sum of OH, HO_2 and H.

ACPD
12, 21065–21104, 2012

HOCl, ClO and HO_2 diurnal variation in the tropics

M. Khosravi et al.

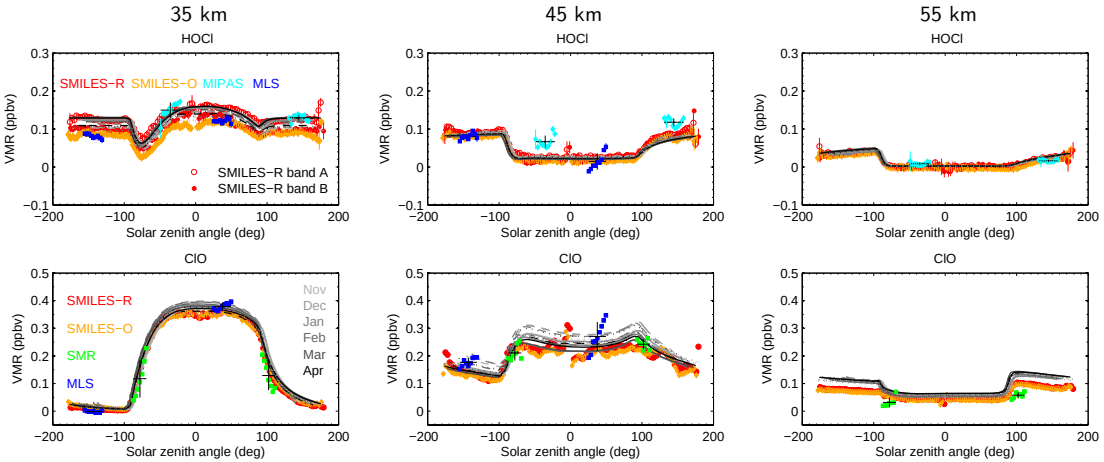

Fig. 3. Modeled diurnal variation of HOCl and ClO at the altitudes 35, 45 and 55 km (left, middle, right) in the tropics between 20° S and 20° N compared to observations made by SMILES, Aura/MLS, Odin/SMR and ENVISAT/MIPAS during the period November 2009 to April 2010. SMILES data are presented by two products; the research product (here called SMILES-R) and the official product (here named SMILES-O). Top row: HOCl; Bottom row: ClO. The standard error of the mean are shown in the same color as the measurements. If not visible, errors are smaller than the symbol size. Model simulations are given for different months (light gray shaded lines: November; dark gray: April). Solid gray lines are for the equator, dotted lines are for 20° S and dashed lines are for 20°N. Satellite data have been averaged in bins of 2.5–3° in terms of solar zenith angle. HOCl data from MIPAS are averaged from November 2003 to April 2004. The model was run with a vertical resolution of 1 km and the model results have been vertically smoothed using 5 and 7 km wide moving averages. MLS, SMR and MIPAS values have been averaged at their ascending/descending nodes. The variability of these measurements in the form of 1-σ standard deviation are shown as vertical error bars in black. The horizontal error bars show the range of solar zenith angles of the respective measurements.

ACPD
12, 21065–21104, 2012

HOCl, ClO and HO_2 diurnal variation in the tropics

M. Khosravi et al.

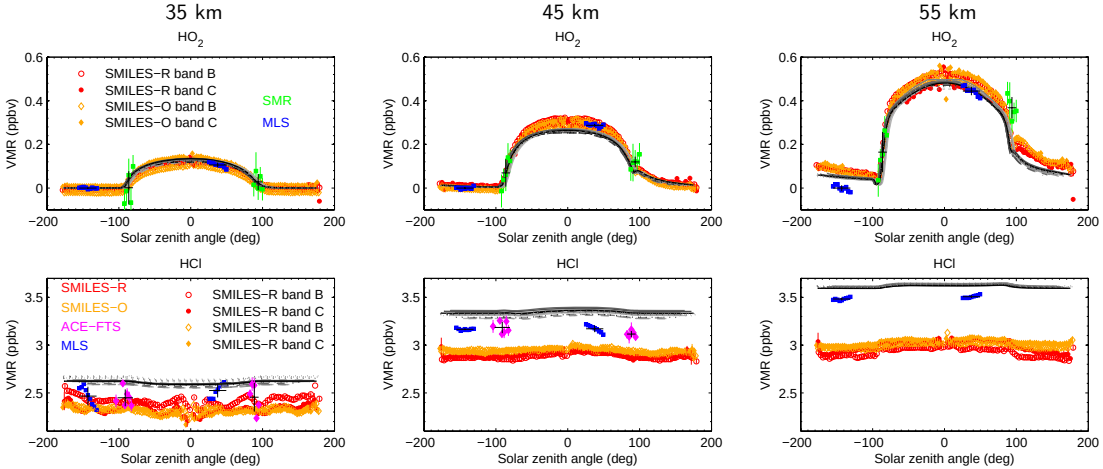

Fig. 4. Same as Fig. 3, but modeled and observed diurnal variation of HO_2 and HCl made by SMILES, Aura/MLS, Odin/SMR and SCISAT/ACE-FTS at the altitudes 35, 45 and 55 km (left, middle, right) during the period November 2009 to April 2010. Top row: HO_2; bottom row: HCl. HO_2 from SMR corresponds to the period October 2003 to October 2004. MLS, SMR and ACE-FTS values have been averaged at their ascending/descending or sunrise/sunset nodes.

ACPD
12, 21065–21104, 2012

HOCl, ClO and HO_2 diurnal variation in the tropics

M. Khosravi et al.

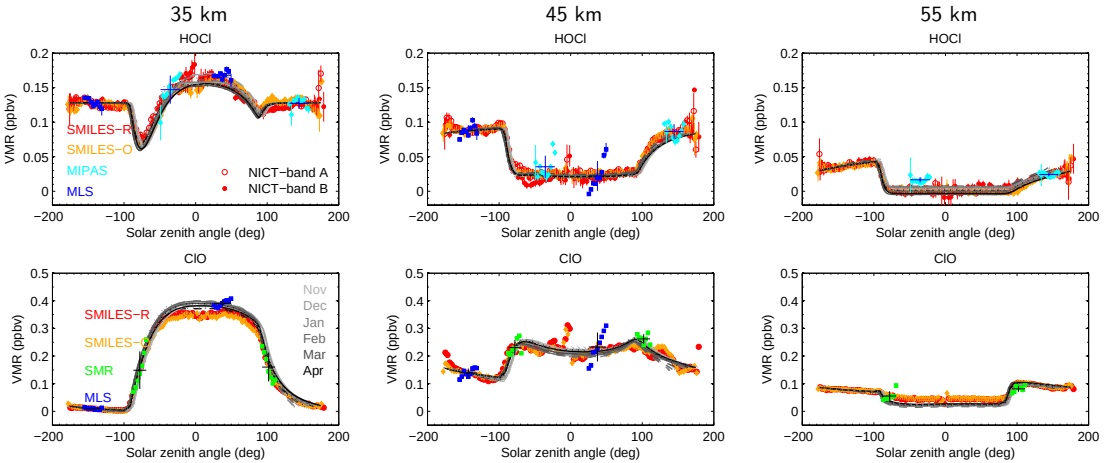

Fig. 5. Same as Fig. 3, but offset shifted for high solar zenith angles at nighttime or sunrise in order to compare the amplitudes of the SMILES, MLS, SMR and MIPAS diurnal cycles with the model. The average nighttime or sunrise satellite measurements in the overlapping solar zenith angles and the model were subtracted from the values at other solar zenith angles and a correction term respective to SMILES-R for the same solar zenith angle range has been added.

ACPD
12, 21065–21104, 2012

HOCl, ClO and HO_2 diurnal variation in the tropics

M. Khosravi et al.

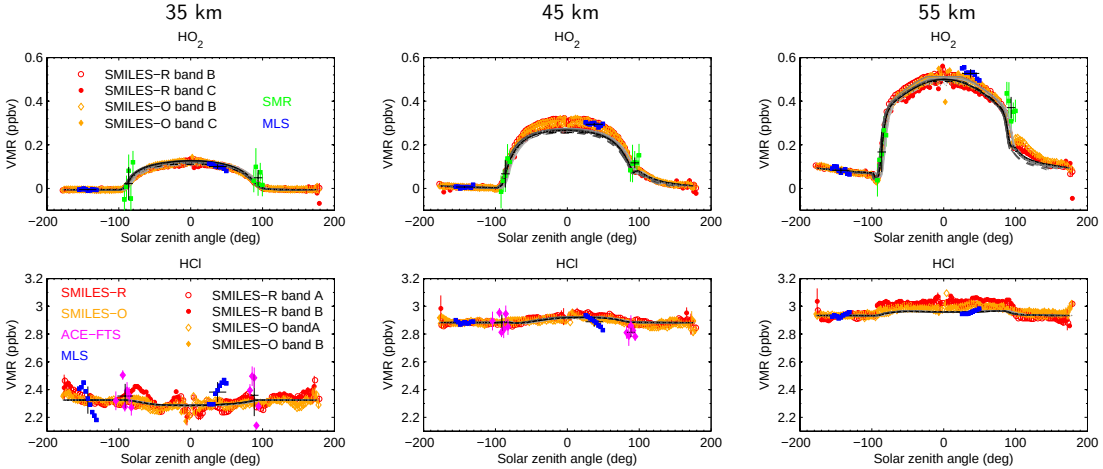

Fig. 6. Same as Fig. 4 but offset shifted for high solar zenith angles at nighttime or sunrise in order to compare the amplitudes of the SMILES, MLS, SMR and ACE-FTS diurnal cycles with the model. The average nighttime or sunrise satellite measurements in the overlapping solar zenith angles and the model were subtracted from the values at other solar zenith angles and a correction term respective to SMILES-R for the same solar zenith angle range has been added.

ACPD
12, 21065–21104, 2012

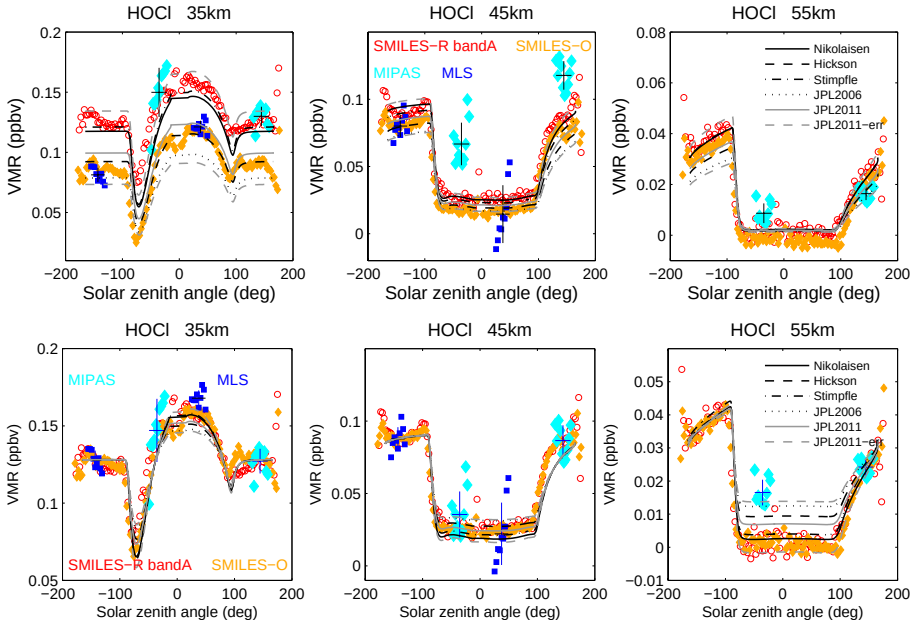

Fig. 7. Sensitivity of the model to different reaction rate constants (k_1) at the altitudes of 35, 45 and 55 km (left, middle and right) for 1 November. The black and gray colors represent the different model simulations using Stimpfle et al. (1979), Nickolaisen et al. (2000), Hickson et al. (2007) as well as JPL 2006 and 2011 recommendations (Sander et al., 2011) for the HOCl formation reaction rate. The simulations for the upper and the lower uncertainty limit of k_1 according to JPL 2011 recommendations are shown as gray dashed lines. Top: observed and modelled volume mixing ratios against solar zenith angle. Bottom: offset shifted observations and model.

ACPD
12, 21065–21104, 2012